PROCEEDINGS OF SCIENCE

The experimental review of $B \to \tau\nu_\tau$, and $B \to D^{(*)}\tau\nu_\tau$ decays.

Andrzej Bozek*
Institute of Nuclear Physics Krakow
E-mail: bozek@belle2.ifj.edu.pl

Experimental studies of B decays to τ leptons, $B \to \tau\nu_\tau$, and $B \to D^{(*)}\tau\nu_\tau$, are reported. The results are based on large data samples collected at the $\Upsilon(4S)$ resonance with the Belle detector at KEKB and the BABAR detector at the SLAC PEP-II asymmetric energy e^+e^- colliders.

Flavor Physics and CP Violation 2010
May 25-29,2010
Turin, Italy

*Speaker.

PoS(FPCP 2010)027

1. Introduction

B decays to τ leptons represent a broad class of processes that can provide interesting tests of the Standard Model (SM) and its extensions. Of particular interest are the modes presented in this report: the purely leptonic decay $B^+ \to \tau^+\nu_\tau$[1, 2, 3, 4] and semi-leptonic decays $B \to D^{(*)}\tau\nu_\tau$[5, 6, 7, 8] [1]. Both decays in the SM occur at tree level.

The purely leptonic decay $B^+ \to \tau^+\nu_\tau$ proceeds via W-mediated annihilation in the SM. It provides a direct determination of the product of B meson decay constant f_B and the magnitude of the Cabibbo-Kobayashi-Maskawa matrix element $|V_{\rm ub}|$. The SM expected branching fraction is $(1.59 \pm 0.40) \times 10^{-4}$ and is given by $\mathscr{B}(B^+ \to \tau^+\nu_\tau) = \frac{G_F^2 m_B m_\tau^2}{8\pi}(1 - \frac{m_\tau^2}{m_B^2})^2 \tau_B f_b^2 |V_{ub}|^2$, where G_F is the Fermi constant, τ_{B^+} is the B^+ lifetime, and m_B and m_τ are the B^+ meson and τ lepton masses.

Theoretical predictions for semileptonic decays to exclusive final states require knowledge of the form factors, which parametrise the hadronic current as functions of $q^2 = (P_B - P_{D^{(*)}})^2$. Branching fractions for semileptonic B decays to τ leptons are predicted to be smaller than those to light leptons. The predicted branching fractions, based on the SM, are around 1.4% and 0.7% for $B^0 \to D^{*-}\tau^+\nu_\tau$ and $B^0 \to D^-\tau^+\nu_\tau$, respectively (see *e.g.*, [9]).

B meson decays with $b \to c\tau\nu_\tau$ and $b \to \tau\nu_\tau$ transitions, due to the large mass of the τ lepton, are sensitive probes of models with extended Higgs sectors[10][11]. In multi-Higgs doublet models, substantial departures from the SM decay rate could occur for $B \to \tau^+\nu_\tau$. The semileptonic B decays to tau provide new observables sensitive to New Physics such as polarizations, which cannot be accessed in leptonic B decays. Also difference to SM decay rate for $B \to D\tau^+\nu_\tau$ can be large. Smaller departures are expected for $B \to D^*\tau^+\nu_\tau$, however they provide cleaner sample and D^* polarisation that can be used to enhance a sensitivity to NP effects.

Difficulties related to multiple neutrinos in the final states cause that there is little experimental information about decays of this type. Prior to the B-factories era, there was only inclusive measurement of $\mathscr{B}(B \to c\tau^+\nu_\tau) = (2.48 \pm 0.26)\%$ from LEP[12].

2. Analysis techniques

At B-factories B decays to multi-neutrino final states can be observed via the recoil of accompanying B meson ($B_{\rm tag}$). The $B_{\rm tag}$ can be reconstructed inclusively from all the particles that remain after selecting $B_{\rm sig}$ candidates or exclusively in several, hadronic or semileptonic decay modes. The remaining charged particles and photons are required to be consistent with the hypothesis that they are coming from $B \to \tau\nu_\tau$ or $B \to D^{(*)}\tau\nu_\tau$ decays. Choice of the τ, D or D^* decay modes, as well as the methods of the $B_{\rm tag}$ reconstruction, depend on particular analysis requirements on purity and signal extraction procedure, etc.

Different tagging techniques have been developed, using full or partial reconstruction of one of the two B mesons in the event to reduce background and improve the determination of kinematic quantities.

[1] Charge conjugate modes are implied throughout this report unless otherwise stated.

2.1 Exclusive reconstruction of $B_{\rm tag}$ in hadronic modes

In BaBar results the $B_{\rm tag}$ candidates are reconstructed in 1114 final states $B_{\rm tag} \to D^{(*)}Y^{\pm}$ with an algorithm that has been used at BaBar for a number of analyses, involving missing momentum[13][2]. These final states arise from the large number of ways to reconstruct the D and D^* mesons within the $B_{\rm tag}$ candidate and the possible pion and kaon combinations within the Y system. The $Y^{\pm}$ system may consist of up to six light hadrons ($\pi^{\pm}, \pi^0, K^{\pm}$, or K_S). In both the $D^{(*)}$ and $Y^{\pm}$ systems, the π^0, K_S^0 and charged kaons are reconstructed and identified employing standart procedures methods available at B-factories.

For Belle case, the $B_{\rm tag}$ candidates are reconstructed in the following decay modes: $B^+_{\rm tag} \to \overline{D}^{(*)0}h^+$, and $B^0_{\rm tag} \to \overline{D}^{(*)-}h^+$, where h^+ can be π^+, ρ^+, a_1^+ or $D_s^{(*)+}$. The a_1^+ candidates are selected by combining a ρ^0 candidate and a pion.

The selection of $B_{\rm tag}$ candidates is based on the energy substituted mass $m_{\rm ES} \equiv \sqrt{E^2_{\rm beam} - p^2_B}$ (see Fig. 1 left) and the energy difference $\Delta E \equiv E_B - E_{\rm beam}$. Here, E_B and p_B are the reconstructed energy and momentum of the $B_{\rm tag}$ candidate in the e^+e^- center-of-mass (CM) system, and $E_{\rm beam}$ is the beam energy in the CM frame.

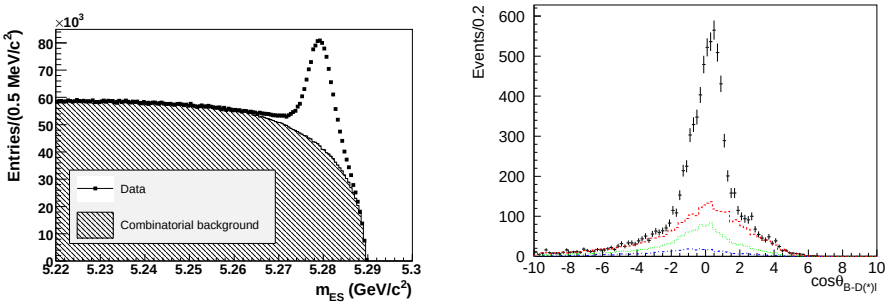

Figure 1: Left: The distribution of the energy substituted mass, $m_{\rm ES}$ (called $m_{\rm bc}$ in Belle), for the $B_{\rm tag}$ candidates in Babar data[2]. The combinatorial background is overlaid. Right: The $\cos\theta_{B-D^{(*)}l}$ distribution, in Belle results[3], for $B^- \to \tau^-\nu_\tau$ candidate events with $E_{\rm ECL} < 1.2$ GeV(see 3.1) selected with all $B_{\rm tag}$ and $B_{\rm sig}$ requirements except for those on $\cos\theta_{B-D^{(*)}l}$. The histograms are the MC expectation for events without $B^+ \to \overline{D}^{(*)0}l^+\nu_l$ decays for different background contributions(See subsection 2.2).

2.2 Exclusive reconstruction of $B_{\rm tag}$ in semi-leptonic decays

The $B_{\rm tag}$ is reconstructed in a set of semileptonic B decay modes $B \to D^{(*)0}X\ell\nu_\ell$, through the full hadronic reconstruction of D^0 mesons and identification of the lepton, $(\ell^- = e, \mu)$. Other particles resulting from a transition from a higher-mass charm state down to the D^0 are not explicitly reconstructed. The $B_{\rm tag}$ candidates are selected using the lepton momentum P_l^* and $\cos\theta_{B-D^{(*)}l}$, the cosine of the angle between the direction of the $B_{\rm tag}$ momentum and the direction of the momentum sum of the $D^{(*)0}\ell$ system (see Fig. 1 right). This angle is calculated using $\cos\theta_{B-D^{(*)}\ell} = (2E_{\rm beam}E_{D^{(*)}\ell} - m_B^2 - m^2_{D^{(*)}\ell})/(2|P_{\rm B}||P_{D^{(*)}\ell}|)$, where $E_{D^{(*)}\ell}$, $P_{D^{(*)}\ell}$, and $m_{D^{(*)}\ell}$ are the energy sum, momentum sum and invariant mass of the $D^{(*)0}$ and lepton, while m_B is the B meson mass.

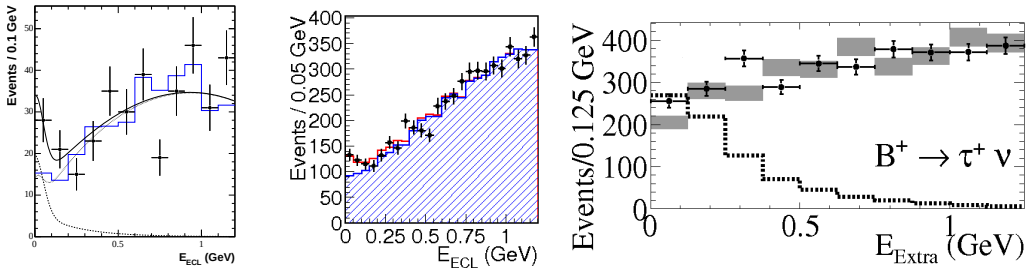

Figure 2: $E_{\rm ECL}$ distribution in data for hadronic tag events in Belle(right) and semileptonic tagged events for Belle results(middle) and BaBar(left). The points with error bars are data. Surimposed are the MC prediction and fit results.

2.3 Inclusive reconstruction of $B_{\rm tag}$ in hadronic modes

The inclusive tagging approach was, up to now, exploited only by Belle collaboration[5, 6].

With this method the reconstruction starts from $B_{\rm sig}$ candidates, reconstruction of $D^{(*)}$ on the signal side strongly suppresses the combinatorial and continuum backgrounds. Once a $B_{\rm sig}$ candidate is found, the remaining particles that are not assigned to $B_{\rm sig}$ are used to reconstruct the $B_{\rm tag}$ decay. The consistency of a $B_{\rm tag}$ candidate with a B-meson decay is checked using the beam-energy constrained mass and the energy difference variables: $M_{\rm tag} = \sqrt{E^2_{\rm beam} - \mathbf{p}^2_{\rm tag}}$, $\mathbf{p}_{\rm tag} = \sum_i \mathbf{p}_i$, and $\Delta E_{\rm tag} = E_{\rm tag} - E_{\rm beam}$, $E_{\rm tag} = \sum_i E_i$, $\mathbf{p}_i$ and E_i denote the 3-momentum vector and energy of the i'th particle. All quantities are evaluated in the $\Upsilon(4S)$ rest frame. The summation is over all particles that are left after reconstruction of $B_{\rm sig}$ candidates.

3. $B^+ \to \tau^+\nu_\tau$

3.1 $B^+ \to \tau^+\nu_\tau$ with hadronic tags

Belle analysis[1] uses a data sample of about 449×10^6 $B\bar{B}$ events with fully reconstructed $B_{\rm tag}$ decays. In this sample, the decays of $B_{\rm sig}$ into a τ and a neutrino is searched; the τ lepton is reconstructed in five decay modes: $\tau^+ \to \mu^+\bar{\nu}_\mu\bar{\nu}_\tau$, $\tau^+ \to e^+\bar{\nu}_e\bar{\nu}_\tau$, $\tau^+ \to \pi^+\bar{\nu}_\tau$, $\tau^+ \to \pi^+\pi^0\bar{\nu}_\tau$ and $\tau^+ \to \pi^+\pi^+\pi^-\bar{\nu}_\tau$, which taken together correspond to 81% of all τ decays. Further requirements on the magnitude and an angular distribution of missing momentum provide background suppression. For the signal side tracks, the momentum $P_{\tau\to X}$ is to be in the region consistent with a $B \to \tau\nu_\tau$ decay. The selection criteria for $B_{\rm tag}$ and $B_{\rm sig}$ are optimised for each of the τ decay modes, because the background levels and the background components are mode-dependent. The remaining energy in the electromagnetic calorimeter, $E_{\rm ECL}$ (or $E_{\rm Extra}$), is the most powerful variable for signal and background separation. It takes values around zero for signal events, while background events are distributed toward higher $E_{\rm ECL}$ due to the contribution from additional neutral clusters.

The signal yield is extracted from a fit to the $E_{\rm ECL}$ distribution (Fig 2). The combined fit for all five τ decay modes gives $17.2^{+5.3}_{-4.7}$ signal events. It corresponds to the branching fraction $\mathscr{B}(B^+ \to \tau^+\nu_\tau) = (1.79^{+0.56}_{-49}(stat)^{+0.46}_{-0.51}(syst)) \times 10^{-4}$. The significance, after including systematic uncertainties, is 3.5σ[2]. This result represents the first evidence of the purely leptonic B decay.

[2]The significance implies inclusions of systematic uncertainties throughout this report.

BaBar collaboration presented a search for the decay $B^+ \to \tau^+\nu_\tau$[2] using 383×10^6 $B\bar{B}$ pairs. They identify the τ lepton in the following modes: $\tau^+ \to e^+\nu_e\bar{\nu_\tau}, \tau^+ \to \mu^+\nu_\mu\bar{\nu_\tau}, \tau^+ \to \pi^+\bar{\nu_\tau}$ and $\tau^+ \to \pi^+\pi^0\bar{\nu_\tau}$. They find 24 events with expected background of 14.27 ± 3.03, which correspond to a 2.2σ excess in data and gives a branching fraction of $\mathscr{B}(B^+ \to \tau^+\nu_\tau) = (1.8^{+0.9}_{-0.8}(stat) \pm 0.4(\text{bck. syst.}) \pm 0.2(\text{other syst.}) \times 10^{-4}$.

3.2 $B^+ \to \tau^+\nu_\tau$ with semileptonic tags

Belle measurement[3] of the decay $B^+ \to \tau^+\bar{\nu_\tau}$ with a semileptonic B tagging method is based a data sample containing 657×10^6 $B\bar{B}$ pairs. The strategy adopted for this analysis is similar to the measurements with hadronic tag. The B_{tag} mesons decaying semileptonically are reconstructed and the properties of the remaining particle(s) in the event are compared to those expected for signal and background.

The signal yield is extracted from a fit to the E_{ECL} distribution (Figure 2). the clear excess of signal events can be observed in the region near $E_{\text{ECL}} \sim 0$. The measured branching fraction is $\mathscr{B}(B^- \to \tau^-\nu_\tau) = (1.54^{+0.38}_{-0.37}(stat)^{+0.29}_{-0.31}(syst)) \times 10^{-4}$ with a significance of 3.8σ. The signal yield is of $n_s = 154^{+36}_{-35}$.

BaBar performed a search[4], with semileptonic tag, for the decay $B^- \to l^-\nu_l$ ($l = \tau, \mu$, or e) in 458.9×10^6 $B\bar{B}$ pairs (see Fig.2). They found $\mathscr{B}(B^- \to \tau^-\nu_\tau) = (1.7 \pm 0.8 \pm 0.2) \times 10^{-4}$, which excludes zero at 2.3σ.

4. $B \to D^{(*)}\tau^+\nu_\tau$

4.1 $B \to D^{(*)}\tau^+\nu_\tau$ with inclusive hadronic tag

Belle collaboration reported the first observation of an exclusive decay with the $b \to c\tau\nu_\tau$ transition[5], in channel $B^0 \to D^{*+}\tau^-\nu_\tau$ observed with B_{tag} reconstructed inclusively in a data sample containing 535×10^6 $B\bar{B}$ pairs. The $\tau^- \to e^-\nu_e\nu_\tau$ and $\tau^- \to \pi^-\nu_\tau$ modes are used to reconstruct τ lepton candidates. The D^{*+} mesons are reconstructed in the $D^{*+} \to D^0\pi^+$ decay channel. The D^0 candidates are reconstructed in the $K^-\pi^+$ and $K^-\pi^+\pi^0$ final states.

To suppress background and improve the quality of the B_{tag} selection, additional requirements are impose like: zero total event charge; no charged leptons in tag side; zero net proton/anti-proton number. The requirements that the candidate events have $-0.3 \text{ GeV} < \Delta E_{\text{tag}} < 0.05 \text{ GeV}$ are applied. These requirements result in flat M_{tag} distributions for most background components , while the distribution of the signal modes peaks, at large missing mass square, at the B mass (See Fig. 3). The main sources of the peaking background are the semileptonic decays $B \to \bar{D}^* l^+\nu_l$ and $B \to \bar{D}^{(*)}\pi l^+\nu_l$ (including $\bar{D}^{**} l^+\nu_l$).

The observed signal of 60^{+12}_{-11} events for the decay $B^0 \to D^{*-}\tau^+\nu_\tau$ with a significance of 5.2σ was extracted from M_{tag} distribution. The corresponding branching fraction is listed in Table1 and is consistent with SM expectations.

A new analysis for $B^+ \to D^{(*)0}\tau^+\nu_\tau$ was performed in a sample of 657×10^6 $B\bar{B}$ pairs[6]. The signal and combinatorial background yields are extracted from an extended unbinned maximum likelihood fit to the M_{tag} and P_{D^0} (momentum of D^0 from B_{sig} measured in the $\Upsilon(4S)$ frame) variables. The $\tau^+ \to e^+\nu_e\nu_\tau$, $\tau^+ \to \pi^+\nu_\tau$, and in addition $\tau^+ \to \mu^+\nu_\tau$ modes are used to reconstruct

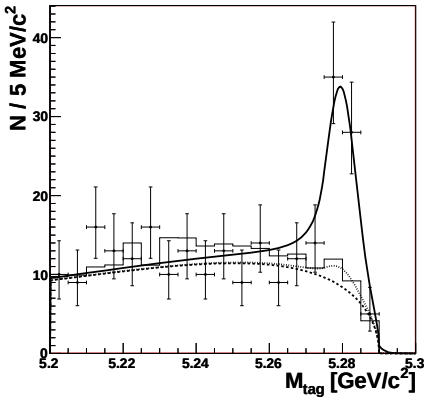

Figure 3: $M_{\rm tag}$ distribution for $B^0 \to D^{*-}\tau^+\nu_\tau$ decay Belle analysis[5]. The histogram represents expected background scaled to the data luminosity. The solid curve shows the result of the fit. The dotted and dashed curves indicate respectively the fitted background and the combinatorial component only.

τ lepton candidates. The D^0 mesons where reconstructed in same way as in the previous analysis. The $\bar{D}^{*0}$ candidates are reconstructed from $\bar{D}^0\pi^0$, where π^0 is reconstructed fully or with one missing γ. In total, 13 different decay chains are considered, eight with $\bar{D}^{*0}$ and five with $\bar{D}^0$ in the final states.

The fits are performed in the range $M_{\rm tag} > 5.2$ GeV/c^2, simultaneously to all data subsets. In each of the sub-channels, the data was described as the sum of four components: signal, cross-feed between $\bar{D}^{*0}\tau^+\nu_\tau$ and $\bar{D}^0\tau^+\nu_\tau$, combinatorial and peaking backgrounds. The common signal branching fractions $\mathscr{B}(B^+ \to \bar{D}^{*0}\tau^+\nu_\tau)$ and $\mathscr{B}(B^+ \to \bar{D}^0\tau^+\nu_\tau)$, and the numbers of combinatorial background in each sub-channel are free parameters of the fit, while the normalisations of peaking background contributions are fixed to the values obtained from the rescaled MC samples. The signal yields and branching fractions for $B^+ \to \bar{D}^{(*)0}\tau^+\nu_\tau$ decays are related assuming equal fractions of charged and neutral B meson pairs produced in $\Upsilon(4S)$ decays. All the intermediate branching fractions are taken from the PDG compilation [12].

The branching fractions extracted from the fit are listed in Table1. The fit projections in $M_{\rm tag}$ and P_{D^0} variables are shown in Fig. 4. The signal yields are 446^{+58}_{-56} $B^+ \to \bar{D}^{*0}\tau^+\nu_\tau$ events and 146^{+42}_{-41} $B^+ \to \bar{D}^0\tau^+\nu_\tau$ events.

4.2 $B \to D^{(*)}\tau^+\nu_\tau$ with exclusive hadronic tags

Babar collaboration presented measurements of the semileptonic decays $B^- \to D^0\tau^-\bar{\nu_\tau}$, $B^- \to D^{*0}\tau^-\bar{\nu_\tau}$, $B^0 \to D^+\tau^-\bar{\nu_\tau}$, $B^0 \to D^+\tau^-\bar{\nu_\tau}$, and $B^0 \to D^{*+}\tau^-\bar{\nu_\tau}$[7]. The data sample consists of 232×10^6 $\Upsilon(4S) \to B\bar{B}$ decays. The events are selected with a D or D^* meson and a light lepton ($= e$ or μ) recoiling against a fully reconstructed B meson. For the $B_{\rm sig}$ meson decaying semileptonically, $D^{(*)}$ candidates are reconstructed in the modes $D^0 \to K^-\pi^+$, $K^-\pi^+\pi^0$, $K^-\pi^+\pi^+\pi$, $K^0_S\pi^+\pi$; $D^+ \to K\pi^+\pi^+$, $K^-\pi^+\pi^+\pi^0$, $K^0_S\pi^+$, $K^-K^+\pi^+$; $D^{*0} \to D^0\pi^0$, $D^0\gamma$; and $D^{*+} \to D^0\pi^+$, $D^+\pi^0$.

The fit is performed to the joint distribution of lepton momentum and missing mass squared, $m^2_{\rm miss}$, to distinguish signal $B \to D^{(*)}\tau^-\nu_\tau(\tau^- \to l^-\bar{\nu_l}\nu_\tau)$ events from the backgrounds, predominantly

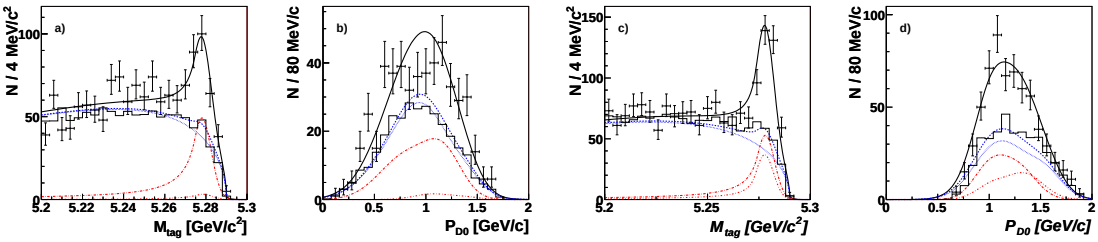

Figure 4: The fit projections to $M_{\rm tag}$, and P_{D^0} for $M_{\rm tag} > 5.26$ GeV$/c^2$ (a,b) for $\bar{D}^{*0}\tau^+\nu_\tau$, (c,d) for $\bar{D}^0\tau^+\nu_\tau$. The black curves show the result of the fits. The solid dashed curves represent the background and the dashed dotted ones show the combinatorial component. The dot-long-dashed and dot-short-dashed curves represent, respectively, the signal contributions from $B^+ \to \bar{D}^{*0}\tau^+\nu_\tau$ and $B^+ \to \bar{D}^0\tau^+\nu_\tau$. The histograms represent the MC-predicted background.

$B \to D^{(*)}\ell^-\bar{\nu}_\ell$. The fit is performed simultaneously in four signal channels.

Figure 5 shows projections in $m^2_{\rm miss}$ for the four signal channels, showing both the low $m^2_{\rm miss}$ region, which is dominated by the normalisation modes $B \to D^{(*)}l\nu_l$, and the high $m^2_{\rm miss}$ region, which is dominated by the signal mode $B \to D^{(*)}\tau\nu_\tau$.

Babar measures the branching-fraction ratios $R(D) = B(B \to D\tau\nu_\tau)/B(B \to Dl\nu_l)$ and $R(D^*) = B(B \to D^*\tau\nu_\tau)/B(B \to D^*l\nu_l)$ and, from a combined fit to B and B^0 channels, approximately 67 $B \to D\tau\nu_\tau$ and 101 $B \to D^*\tau\nu_\tau$ signal events where observed, corresponding to resulting ratios $R(D) = (41.6 \pm 11.7 \pm 5.2)\%$ and $R(D^*) = (29.7 \pm 5.6 \pm 1.8)\%$, where the uncertainties are statistical and systematic. The signal significances are 3.6σ and 6.2σ for $R(D)$ and $R(D^*)$, respectively. Normalising to world averaged $B^- \to D^{(*)0}l^-\nu_l$ branching fractions[12], they obtain $B(B \to D^*\tau\nu_\tau) = (0.86 \pm 0.24 \pm 0.11 \pm 0.06)\%$ and $B(B \to D^*\tau\nu_\tau) = (1.62 \pm 0.31 \pm 0.10 \pm 0.05)\%$, where the additional third uncertainty is from the normalisation mode. They present for the first time, distributions of the lepton momentum, $|p^*_l|$(Fig.5), and the squared momentum transfer, q^2. The measured branching-fraction ratios for individual $D^{(*)}$ states are sumurised in Table2.

Belle collaboration presented similar study based on 604.5 fb^1 of the data sample[8]. The $B \to D\tau\nu_\tau$ and $B \to D^*\tau\nu_\tau$ signals are extracted using unbinned extended maximum likelihood fits to the two-dimensional $(m^2_{\rm miss}, E^{\rm ECL}_{\rm extra})$ distributions obtained after the selection of the signal decays. The B^+ and B^0 samples are fitted separetly. The cross talk between the two tags is found to be small. Then for each B^0 and B^+ tag, a fit is performed simultaneously to the two distributions for the $D\tau\nu_\tau$ and $D^*\tau\nu_\tau$. The fit components are two signal modes; $B \to D\tau\nu_\tau$ and $B \to D^*\tau\nu_\tau$, and the backgrounds from $B \to D\ell\nu_e$, $B \to D^*\ell\nu_e$ and other processes. For the fitting of the $B^0 \to D^{*-}\tau^+\nu_\tau$ distribution, the $D\tau\nu_\tau$ cross feed and $D\ell\nu_\ell$ background are not included, because their contribution are found to be small. The fit region is defined by $(-2 < m^2_{\rm miss}({\rm GeV}^2/c^4) < 8, 0 < E^{\rm ECL}_{\rm extra}({\rm GeV}) < 1.2)$ for all the four signal modes.

The two-dimensional PDF's for $D^{(*)}\tau\nu_\tau$ and $D^{(*)}\ell\nu_l$ processes are created by taking the product of one-dimensional PDF for each variable, as correlation between $m^2_{\rm miss}$ and $E^{\rm ECL}_{\rm extra}$ for these processes are found to be small in the MC simulation. The PDF for the other background processes is made by using the two-dimensional histograms obtained by the MC simulation, since correlation

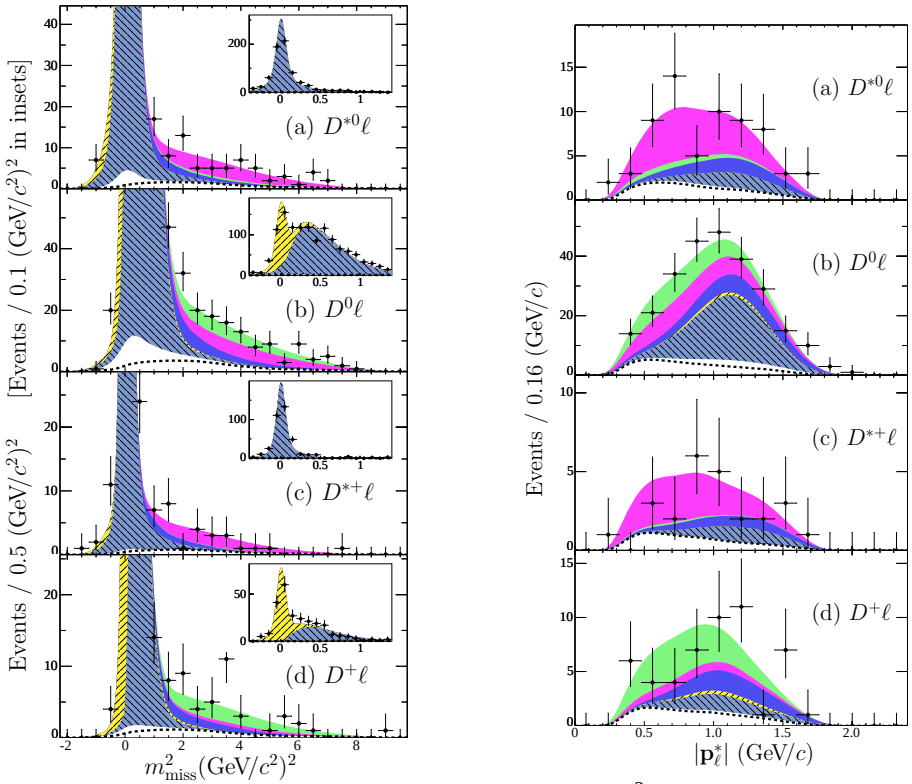

Figure 5: Distributions of events and fit projections in $m^2_{\rm miss}$(left) and in $|P^*_l|$ for the four final states: $D^{*0}l^-$, D^0l^-, $D^{*+}l^-$, and D^+l^-. The normalisation region $m^2_{\rm miss} \approx 0$ is shown with finer binning in the insets. The $|P^*_l|$ is shown in the signal region, $m^2_{\rm miss} > 1(GeV/c^2)^2$. The fit components are combinatorial background (white, below dashed line), charge-crossfeed background (white, above dashed line), the $B \to Dl\nu_l$ normalisation mode (// hatching, yellow), the $B \to D^*l\nu_l$ normalisation mode (\\hatching, light blue), $B \to D^{**}l\nu_l$ background (dark, or blue), the $B \to D\tau\nu_\tau$ signal (light grey, green), and the $B \to D^*\tau\nu_\tau$ signal (medium grey, magenta).

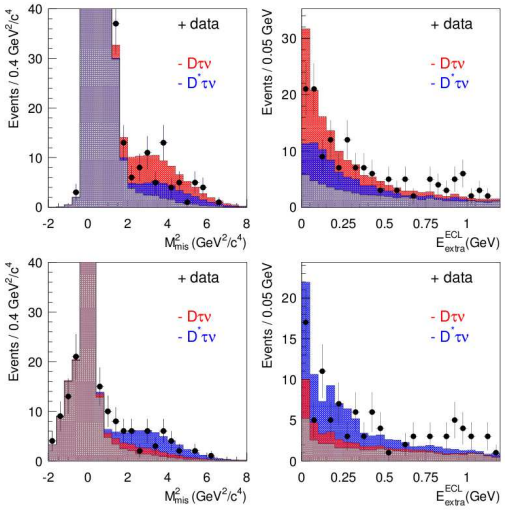

Figure 6: Fit results for $B^+ \to \overline{D}^0\tau^+\nu_\tau$ (top) and $B^+ \to \overline{D}^{*0}\tau^+\nu_\tau$ (bottom). The $m^2_{\rm miss}$ (left) and $E^{\rm ECL}_{\rm extra}$ (right) distributions are shown with the signal selection cut on the other variable[8].

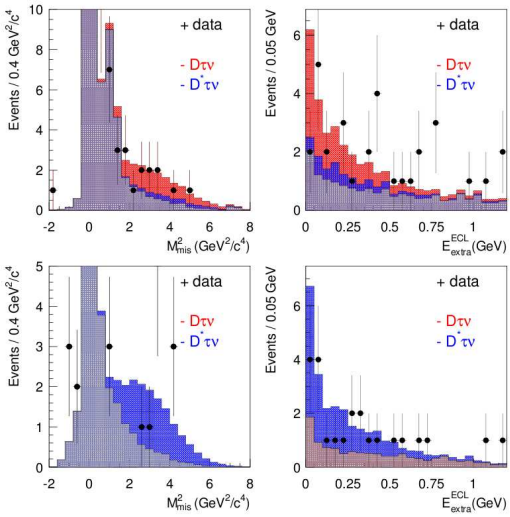

Figure 7: Fit results for $B^0 \to D^-\tau^+\nu_\tau$ (top) and $B^0 \to D^{*-}\tau^+\nu_\tau$ (bottom). The $m^2_{\rm miss}$ (left) and $E^{\rm ECL}_{\rm extra}$ (right) distributions are shown with the signal selection cut on the other variable[8].

between the two variables is significant for these background processes, which mainly come from hadronic B decays.

Figures 6 and 7 show the fit results for $B^+ \to D^{(*)0}\tau\nu_\tau$ and $B^0 \to D^{(*)-}\tau\nu_\tau$, respectively. The results for the four ratios are listed in Table2,

Taking into account the branching fractions for the $B \to D^*\ell\nu_l$ normalisation decays, reported in [12] , the branching fractions for the $B \to D^*\tau\nu_\tau$ decays are obtained and listed in Table1.

4.3 Summary of $B \to D^{(*)}\tau^+\nu_\tau$

Table 1: Summary of branching-fractions for $B \to D^{(*)}\tau\nu_\tau$ decays([%]), where the first error is statistical, the second is systematic, and the third is due to the branching fraction error for the normalisation modes. In brackets are significances, after including the systematics($[\sigma]$).

Mode	Belle[5][6]	BaBar[7]	Belle[8]
$B^+ \to \overline{D}^{*0}\tau^+\nu_\tau$	$2.12^{+0.28}_{-0.27} \pm 0.29(8.1)$	$2.25 \pm 0.48 \pm 0.22 \pm 0.17(5.3)$	$3.04\ ^{+0.69}_{-0.66}\ ^{+0.40}_{-0.47} \pm 0.22(3.9)$
$B^0 \to D^{*-}\tau^+\nu_\tau$	$2.02^{+0.40}_{-0.37} \pm 0.37(5.2)$	$1.11 \pm 0.51 \pm 0.04 \pm 0.04(2.7)$	$1.51\ ^{+0.41}_{-0.39}\ ^{+0.24}_{-0.19} \pm 0.15(4.7)$
$B^+ \to \overline{D}^0\tau^+\nu_\tau$	$0.77 \pm 0.22 \pm 0.12(3.5)$	$0.67 \pm 0.37 \pm 0.11 \pm 0.07(1.8)$	$1.01\ ^{+0.46}_{-0.41}\ ^{+0.13}_{-0.11} \pm 0.10(3.8)$
$B^0 \to D^-\tau^+\nu_\tau$	-	$1.04 \pm 0.35 \pm 0.15 \pm 0.10(3.3)$	$2.56\ ^{+0.75}_{-0.66}\ ^{+0.31}_{-0.22} \pm 0.10(2.6)$

Table 2: The measured branching-fraction ratios for individual $D^{(*)}$ states for analysis based on exclusive $B_{\rm tag}$ reconstruction.The first errors are the statistical and the second errors are the systematic.

	BaBar[7]	Belle[8]
$R(\overline{D}^0)$	$(31.4 \pm 17.0 \pm 4.9)\%$	$(70\ ^{+19}_{-18}\ ^{+11}_{-9})\%$
$R(\overline{D}^{*0})$	$(34.6 \pm 7.3 \pm 3.4)\%$	$(47\ ^{+11}_{-10}\ ^{+6}_{-7})\%$
$R(D^-)$	$(48.9 \pm 16.5 \pm 6.9)\%$	$(48\ ^{+22}_{-19}\ ^{+6}_{-5})\%$
$R(D^{*-})$	$(20.7 \pm 9.5 \pm 0.8)\%$	$(48\ ^{+14}_{-12}\ ^{+6}_{-4})\%$

The current experimental status of semi tauonic B decays is summrized in Table 1.

There is no yet HFAG experimental average of the semi-tauonic B decays. Taking into account all available experimental results from Belle and Babar a naive weighted averages can be calculated[3]:

- $\mathscr{B}(B^+ \to \overline{D}^{*0}\tau^+\nu_\tau) = (2.36 \pm 0.27)\%$
- $\mathscr{B}(B^0 \to D^{*-}\tau^+\nu_\tau) = (1.70 \pm 0.34)\%$
- $\mathscr{B}(B^+ \to \overline{D}^0\tau^+\nu_\tau) = (0.89 \pm 0.20)\%$
- $\mathscr{B}(B^0 \to D^-\tau^+\nu_\tau) = (1.03 \pm 0.30)\%$

Experimentally all modes are clearly established, with significance at least 3σ (over 5σ for D^* modes). They are observed in both experiments and there is still a room for improvement since the results are not based on full statistics.

[3] it takes into account correlations in systematic for Belle results

5. Summary

The studies of B decays to τ at B-factories brought significant advances in this field, providing the first evidence of the purely leptonic $B^+ \to \tau^+\nu_\tau$ mode, semi-tauonic $B \to D\tau^+\nu_\tau$ modes and the observation of semi-tauonic B decays in the $B \to D^*\tau^+\nu_\tau$ channels. These results are consistent with the SM but, given the uncertainties, there is still a room for a sizeable non-SM contribution. The Super B-factories with ≈ 50 times higher statistics should measure these modes with much higher precision. Of particular interest will be measurements of differential distributions.

References

[1] Ikado K *et al.* (Belle Collaboration) 2006 *Phys. Rev. Lett.* **97** 251802

[2] Aubert B *et al.* (Babar Collaboration) 2008 *Phys. Rev. D Rapid Communications* **77** 011107

[3] Hara K *et al.* (Belle Collaboration) 2010 *Phys. Rev. D* **82** 071101

[4] Aubert B *et al.* (Babar Collaboration) 2009 *Phys. Rev. D* **79** 092002; 2010 *Phys. Rev. D Rapid Communications* **81** 051101

[5] Matyja A *et al.* (Belle collaboration), *Phys. Rev. Lett.* **99**, 191807

[6] Bozek A *et al.* (Belle Collaboration)*Phys. Rev. D* bf 82, 072005 (2010)

[7] Aubert B *et al.* (Babar Collaboration) 2009 *Phys. Rev. D* **79** 092002; PRL 100, 021801 (2008); 2008 *Phys. Rev. Lett.* **100** 021801

[8] Adachi I *et al.* (Belle Collaboration)hep-ex/0910.4301

[9] C.-H. Chen and C.-Q. Geng, JHEP 0610, 053 (2006).

[10] Hou W S 1993 *Phys. Rev. D* **48** 2342

[11] Itoh H, Komine S and Okada Y 2005 *Progr. Theor. Phys.* **114** 179 and references therein;

[12] C. Amsler *et al.* (Particle Data Group), Phys. Lett. B **667**, 1 (2008).

[13] B. Aubert et al. (BaBar Collaboration), *Phys. Rev. Lett.* **92**, 071802 (2004); *Phys. Rev. Lett.* **93** 091802 (2004); *Phys. Rev. D* **69**, 111103 (2004); *Phys. Rev. D* **69**, 111104 (2004); *Phys. Rev. Lett.* **94**, 101801 (2005); *Phys. Rev.Lett.* **96**, 241802 (2006); *Phys. Rev. Lett.* **99**, 201801 (2007); *Phys. Rev. D* **77**, 011104 (2008); *Phys. Rev. D* 77, 032007 (2008); *Phys. Rev. D* **77**, 051103 (2008); *Phys. Rev. Lett.* **100**, 151802 (2008); *Phys. Rev. Lett.* **100**, 171802 (2008).